

Dynamic Conductivity and "Coherence Peak" in $\text{YBa}_2\text{Cu}_3\text{O}_7$ Superconductors

Martin C. Nuss, P. M. Mankiewich,^(a) M. L. O'Malley, and E. H. Westerwick
AT&T Bell Laboratories, Crawfords Corner Road, Holmdel, New Jersey 07733

Peter B. Littlewood
AT&T Bell Laboratories, 600 Mountain Avenue, Murray Hill, New Jersey 07974
 (Received 9 April 1991)

We measure directly both the real and imaginary parts of the sub-band-gap conductivity σ in $\text{YBa}_2\text{Cu}_3\text{O}_7$ in the 15–80 cm^{-1} frequency range using coherent time-domain terahertz spectroscopy. We observe a peak in the real part σ_1 similar to the coherence peak expected in an s -wave BCS superconductor. The absence of such a peak in NMR relaxation-rate experiments suggests that its origin lies in a strongly temperature-dependent inelastic-scattering rate rather than in coherence factors.

PACS numbers: 74.30.Gn, 74.70.Vy, 78.47.+p, 84.40.Cb

Measurements of the dynamic response of conventional superconductors have played a crucial role in understanding the origin of superconductivity and in establishing the microscopic Bardeen-Cooper-Schrieffer¹ (BCS) theory of superconductivity. For instance, far-infrared transmission and reflectivity measurements provided the existence proof for the superconducting energy gap in lead² and indications for strong-coupling effects in NbN films.³ In the high-temperature superconductors, reflectivity measurements on $\text{YBa}_2\text{Cu}_3\text{O}_7$ single crystals and films^{4–6} as well as transmission measurements on $\text{Bi}_2\text{Sr}_2\text{CaCu}_2\text{O}_8$ cleaved crystals⁷ have been performed, but unfortunately with widely diverging results and interpretations.

In this Letter, we present measurements of both the real and imaginary parts of the conductivity σ of high-quality superconducting $\text{YBa}_2\text{Cu}_3\text{O}_7$ films in the frequency range from 500 GHz to 2.5 THz (15–80 cm^{-1}) by coherent time-domain terahertz spectroscopy. Unlike conventional Fourier-transform far-infrared spectroscopy, owing to its phase sensitivity, this technique permits us to measure both the real and imaginary parts of the conductivity simultaneously without referring to the Kramers-Kronig relations. Furthermore, we can study thin superconducting films in transmission, which offers greatly increased accuracy compared to reflection measurements, where the reflectivity is close to unity for energies below the gap.

This novel spectroscopic technique has recently been successfully applied to the measurement of the conductivity of doped semiconductors,⁸ the absorption coefficient and refractive index of dielectrics,⁹ the measurement of the superconducting band gap in niobium films,¹⁰ as well as the surface impedance of $\text{YBa}_2\text{Cu}_3\text{O}_7$ superconducting films.¹¹

The setup of our coherent time-domain spectrometer is similar to the one described earlier,^{10,11} but includes additional focusing optics for small samples. It resembles a conventional spectrometer, but here the electromagnetic far-infrared radiation is generated and detected by time-resolved optoelectronic techniques, which results in

the phase sensitivity of the technique. Both source and detector consist of 50- μm dipole antennas with integrated radiation-damaged silicon-on-sapphire photoconductive switches.¹² The transmitter antenna, which is biased with a dc voltage, emits a short electromagnetic burst with a broad frequency spectrum extending from almost dc to more than 2.5 THz when the 100-fs optical pulse from a colliding-pulse mode-locking dye laser switches the photoconductive dipole.¹² On the receiver side, the photoconductive switch operates in a sampling mode and measures the transient photocurrent received by the dipole antenna. Thus, scanning the time delay between the two femtosecond optical pulses yields the temporal shape of the electromagnetic pulse propagated from transmitter to receiver. The sample is placed inside a continuous-flow cryostat equipped with high-resistivity silicon windows at the focal point in the center of the setup.

A 500- \AA -thick superconducting $\text{YBa}_2\text{Cu}_3\text{O}_7$ film is deposited by multiple-electron-beam coevaporation of Y, Cu, and BaF_2 onto a 0.5-mm-thick LaAlO_3 substrate and postannealed in wet oxygen at 850 °C.¹³ This film is optically smooth and oriented with the c axis of the $\text{YBa}_2\text{Cu}_3\text{O}_7$ normal to the substrate surface. We measure a room-temperature resistivity of 160 $\mu\Omega\text{cm}$ that extrapolates to zero at 0 K, and a transition temperature of 91 K.

The frequency response of the superconducting $\text{YBa}_2\text{Cu}_3\text{O}_7$ films is obtained from the time-domain data by Fourier transformation. For thin films with thickness d small compared to the penetration depth λ of the electromagnetic fields, the boundary conditions at the interface between air and the substrate of index n supporting the thin superconducting film can be solved to yield the transmission coefficient for perpendicular incidence:

$$E_t = \frac{2}{1+n+Z_0\sigma_s} E_i, \quad (1)$$

where E_i, E_t are the Fourier components of the incident and transmitted fields, Z_0 is the impedance of free space, and σ_s is the surface conductivity in Ω^{-1} . To eliminate the influence of the small but not negligible substrate ab-

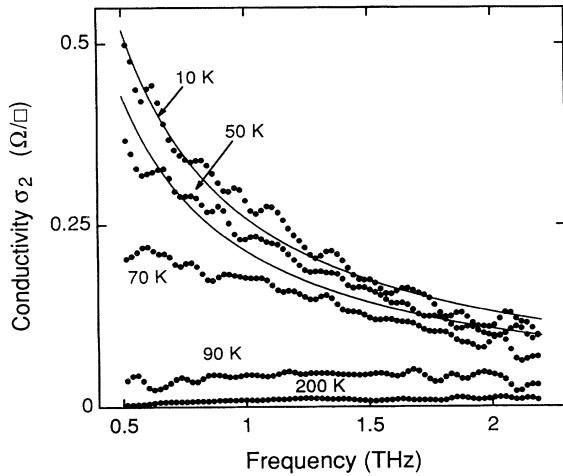


FIG. 1. Imaginary part σ_2 of the conductivity. The solid lines at the two lowest temperatures show fits by a $1/\omega$ frequency dependence.

sorption and dispersion,¹⁴ as well as the influence of the second surface at the back of the substrate, we define a transmission coefficient $t'(\omega)$ referenced with respect to the transmitted field E_t^0 through the substrate alone, i.e., without superconducting film:

$$t' = \frac{E_t}{E_t^0} = \frac{1+n}{1+n+Z_0\sigma_s}. \quad (2)$$

For the reference wave forms through the substrate alone, the superconducting film is etched off after recording the time-domain data at all temperatures and the transmission is measured again without the film at each temperature, going through the same section of the substrate as before. We then obtain the complex conductivity of the superconducting film using Eq. (2).

Figures 1 and 2 show the results for the imaginary part σ_2 and the real part σ_1 , respectively. σ_2 rises monotonically from a small value of 200 K, until at 10 K, σ_2 exhibits a $1/\omega$ dependence, which is shown by the solid lines in Fig. 1. In local electrodynamics, the imaginary part of the conductivity is described by $\sigma_2 = 1/\omega\mu_0\lambda^2$ at $T=0$ regardless of the microscopic theory, which allows us to determine the magnetic penetration depth from the data at low temperature. At 10 K, we obtain $\lambda = 1600$ Å, in excellent agreement with independent penetration-depth measurements on $\text{YBa}_2\text{Cu}_3\text{O}_7$ single crystals and films.^{15,16} The good fit of the $1/\omega$ curve to the data at 10 K also shows that the penetration depth is not dependent on frequency at this temperature.

Figure 2 plots the absorptive part σ_1 of the conductivity. The solid lines are guides to the eye and have a logarithmically diverging frequency dependence. Although this is the frequency dependence predicted by the Mattis-Bardeen theory, the agreement is probably coincidental. Starting from the normal state, σ_1 initially rises with decreasing temperature up to a temperature of

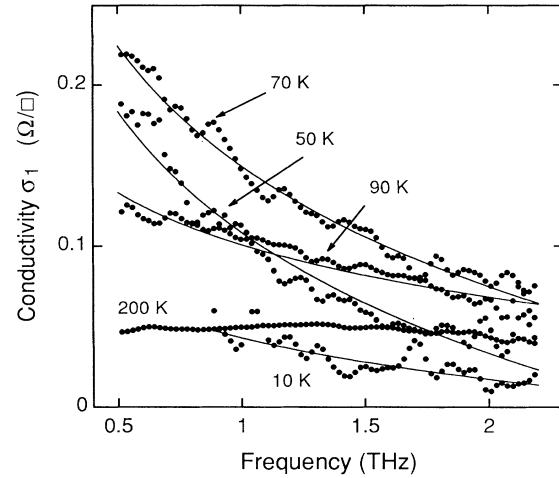


FIG. 2. Real part σ_1 of the conductivity. Solid lines are guides to the eye.

roughly 70 K, but then becomes smaller again. To investigate the temperature dependence in more detail, we plot σ_1 as a function of temperature for three different frequencies (Fig. 3). At all frequencies, σ_1 rises above the normal-state value and exhibits a peak at roughly 70 K. The magnitude of the peak becomes smaller at higher frequencies, in agreement with recent measurements above 200 cm^{-1} (6 THz), where a peak in the conductivity was not observed.¹⁷ At low temperature, we expect σ_1 to vanish exponentially because of the vanishing density of states. However, error bars at low temperature are much higher than for temperatures above 40 K since σ_2 dominates the transmission coefficient there, and we cannot confirm this behavior. Furthermore, σ_1 at the lowest temperatures may be limited by residual absorption processes and not by intrinsic excitation phenomena.

The behavior of σ_1 shown in Fig. 3 is similar to that

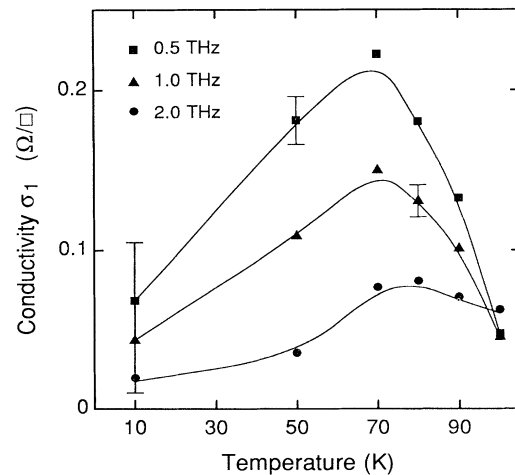


FIG. 3. Temperature dependence of σ_1 for frequencies of 500 GHz, 1 THz, and 2 THz. The solid lines are guides to the eye.

expected from absorption processes involving type-II coherence factors, predicted within the BCS theory for both the conductivity and the nuclear relaxation rate T_1^{-1} .¹⁸ In $\text{YBa}_2\text{Cu}_3\text{O}_7$, however, measurements of T_1^{-1} have not shown the Hebel-Slichter peak.^{19,20} The absence of the NMR coherence peak has been attributed to strong pair breaking close to T_c which smears the singular BCS density of states.^{21,22} Since this argument applies to σ_1 as well, it is likely that the peak in the conductivity observed in our data has a different origin.

The proportionality of T_1^{-1} and σ_1 at low frequencies $\omega \ll 2\Delta$ is only expected in the dirty limit, when the quasiparticle lifetime τ is short ($< \Delta^{-1}$) and independent of temperature.²³ This is unlikely to be the case here because of the strong T -dependent inelastic scattering that dominates the transport properties above T_c . Many of the unusual normal-state properties can be traced to strong scattering from low-energy spin and charge fluctuations, with a flat spectrum extending to energy scales $\sim kT$.^{24,25} In the superconducting state, these low-energy fluctuations are expected to develop a gap of roughly 2Δ , and thus the low-energy scattering of quasiparticles will be suppressed. In consequence, the quasiparticle lifetime τ will grow rapidly. A peak in $\sigma_1(T)$ may arise as T is lowered because of a competition between the growing lifetime and a lowering density of states.

We have modeled this behavior by solving the Eliashberg equations with a spectrum of excitations of the form $\alpha^2 F(\omega) = \lambda \tanh(\omega/2T) N_2(\omega) [1 + (\omega/\omega_0)^2]^{-1}$. (3)

Here λ is the coupling constant, N_2 is the joint density of states for quasiparticle-hole pairs (constant in the normal state and with a gap 2Δ at low temperatures), and ω_0 is a high-frequency cutoff. We have given details of this procedure elsewhere.²⁵ Similar calculations have been carried out by Nicol, Carbotte, and Timusk.²⁶ The results are shown in Fig. 4, for the parameters $\lambda = 0.3$, $\omega_0 = 1000 \text{ cm}^{-1}$, consistent with normal-state transport data; we find $T_c \sim 100 \text{ K}$ and $2\Delta(0)/T_c = 4.2$. In the same figure, we also plot the calculated T_1^{-1} , which shows no "coherence" peak, whereas the low-frequency conductivity is strongly enhanced. The calculations should be used only for qualitative comparison, as we have made no attempt to vary parameters to improve the agreement with the experiment. Moreover, the specific choice of the cutoff function in Eq. (3) influences the details in the shapes of the curves (both in the position and magnitude of the peaks).

There are other experimental consequences of this picture. The onset of continuum Drude-like absorption at zero temperature will be near 4Δ in the clean limit,^{25,27} instead of the conventional value of 2Δ . This is because the quasiparticle lifetime is infinite at low energies, and is finite only above an energy 2Δ from the bottom of the band (i.e., 3Δ above the chemical potential). This onset

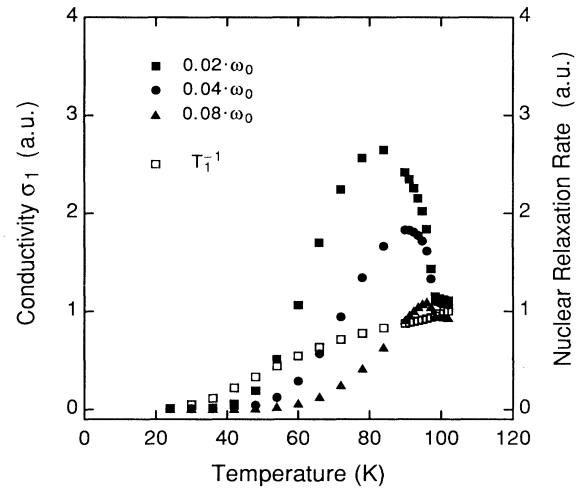


FIG. 4. Temperature dependence of σ_1 within the marginal Fermi-liquid theory for $\lambda = 0.3$, $2\Delta/T_c = 4.2$, and $\Delta = 0.17\omega_0$. The solid symbols indicate σ_1 at various sub-band-gap frequencies, the open symbols the temperature dependence of the nuclear relaxation rate T_1^{-1} .

is expected to be visible in spectroscopic techniques, and may already have been observed in tunneling^{28,29} and photoemission.³⁰ There may also be a peak in the *electronic* thermal conductivity below T_c , even though this is not expected within BCS because of the type-I coherence factors; here it can arise from the same lifetime effects that cause the peak in σ_1 .

We would like to mention that recent microwave experiments³¹ have been interpreted as showing an even sharper feature in σ_1 than we observe here (albeit at somewhat lower frequency). These results are difficult to reconcile with the present data.

In conclusion, we have shown that unlike the nuclear relaxation rate T_1^{-1} , the real part of the conductivity σ_1 in $\text{YBa}_2\text{Cu}_3\text{O}_7$ superconductors exhibits a coherence peak in the superconducting state. However, the assignment as a coherence peak is misleading, since the strongly decreasing inelastic-scattering rate below T_c causes the peak in σ_1 , not interference terms in the quasiparticle wave functions of a Cooper pair. In the framework of the marginal Fermi-liquid phenomenology, the inelastic-scattering rate enters σ_1 , but not the nuclear relaxation rate T_1^{-1} , explaining the absence of a peak in the NMR data. We employ the marginal Fermi-liquid phenomenology because it is convenient; however, we stress that the qualitative behavior will be reproduced by any model in which low-energy quasiparticle scattering is suppressed in the superconductor. Besides the strong temperature dependence of the scattering rate, mainly the smearing of the density of states around the gap energy Δ is responsible for the differences between the coherence peak observed in conventional superconductors and the peak in σ_1 reported here. Finally, our results imply that

the quasiparticle scattering rate is strongly suppressed in the superconducting state and should lay to rest any lingering suspicion that the anomalous behavior of high- T_c materials can be ascribed to strong electron-phonon coupling.

^(a)Also at Boston University, Boston, MA 02215.

- ¹J. Bardeen, L. N. Cooper, and J. R. Schrieffer, *Phys. Rev.* **108**, 1175 (1957).
- ²L. H. Palmer and M. Tinkham, *Phys. Rev.* **165**, 588 (1968).
- ³D. R. Karecki, G. L. Carr, S. Perkowitz, D. U. Gubser, and S. A. Wolf, *Phys. Rev. B* **27**, 5460 (1983).
- ⁴J. S. Orenstein, G. A. Thomas, A. J. Millis, S. L. Cooper, D. H. Rapinke, T. Timusk, L. F. Schneemeyer, and J. V. Waszczak, *Phys. Rev. B* **42**, 6342 (1990).
- ⁵Z. Schlesinger, R. T. Collins, F. Holtzberg, C. Feild, S. H. Blanton, U. Welp, G. W. Crabtree, and Y. Fang, *Phys. Rev. Lett.* **65**, 801 (1990).
- ⁶K. Kamaras, S. L. Herr, C. D. Porter, N. Tache, D. B. Tanner, S. Etemad, T. Venkatesan, E. Chase, A. Inam, X. D. Wu, M. S. Hedge, and B. Dutta, *Phys. Rev. Lett.* **64**, 84 (1990).
- ⁷L. Forro, G. L. Carr, G. P. Williams, D. Mandrus, and L. Mihaly, *Phys. Rev. Lett.* **65**, 1941 (1990).
- ⁸M. van Exter and D. Grischkowsky, *Phys. Rev. B* **41**, 12140 (1990).
- ⁹D. Grischkowsky, S. Keiding, M. van Exter, and C. Fattinger, *J. Opt. Soc. Am. B* **7**, 2006 (1990).
- ¹⁰M. C. Nuss, K. W. Goossen, J. P. Gordan, P. M. Mankiewich, M. L. O'Malley, and M. Bhushan (to be published).
- ¹¹M. C. Nuss, K. W. Goossen, P. M. Mankiewich, and M. L. O'Malley, *Appl. Phys. Lett.* **58**, 2561 (1991).
- ¹²P. R. Smith, D. H. Auston, M. C. Nuss, *IEEE J. Quantum Electron.* **24**, 255 (1988).
- ¹³P. M. Mankiewich, R. E. Howard, W. J. Skocpol, A. H. Dayem, A. Ourmazd, M. G. Young, and E. Good, in *High Temperature Superconductors I*, edited by M. B. Brodsky *et al.*, MRS Symposium Proceedings Vol. 99 (Materials Research Society, Pittsburgh, PA, 1988), pp. 119–125.
- ¹⁴D. Grischkowsky and S. Keiding, *Appl. Phys. Lett.* **57**, 1055 (1990).
- ¹⁵D. R. Harshman, L. F. Schneemeyer, J. V. Waszczak, G. Aeppli, R. J. Cava, B. Batlogg, L. W. Rupp, E. J. Ansaldo, and D. L. Williams, *Phys. Rev. B* **39**, 851 (1989).
- ¹⁶A. T. Fiory, A. F. Hebard, P. M. Mankiewich, and R. E. Howard, *Phys. Rev. Lett.* **61**, 1419 (1988).
- ¹⁷R. T. Collins, Z. Schlesinger, F. Holtzberg, C. Feild, U. Welp, G. W. Crabtree, J. Z. Liu, and Y. Fang, *Phys. Rev. B* **43**, 8701 (1991).
- ¹⁸L. C. Hebel and C. P. Slichter, *Phys. Rev.* **113**, 1504 (1959).
- ¹⁹R. E. Walstedt, W. W. Warren, R. F. Bell, G. F. Brennert, G. P. Espinosa, R. J. Cava, L. F. Schneemeyer, and J. V. Waszczak, *Phys. Rev. B* **38**, 9299 (1988).
- ²⁰P. C. Hammel, M. Takigawa, R. H. Heffner, Z. Fisk, and K. C. Ott, *Phys. Rev. Lett.* **63**, 1992 (1989).
- ²¹Y. Kuroda and C. M. Varma, *Phys. Rev. B* **42**, 8619 (1990).
- ²²L. Coffey, *Phys. Rev. Lett.* **64**, 1071 (1990).
- ²³D. C. Mattis and J. Bardeen, *Phys. Rev.* **111**, 412 (1958).
- ²⁴C. M. Varma, P. B. Littlewood, S. Schmitt-Rink, E. Abrahams, and A. E. Ruckenstein, *Phys. Rev. Lett.* **63**, 1996 (1989); **64**, 497(E) (1990).
- ²⁵P. B. Littlewood and C. M. Varma, *J. Appl. Phys.* **69**, 4979 (1991).
- ²⁶E. J. Nicol, J. P. Carbotte, and T. Timusk, *Phys. Rev. B* **43**, 473 (1991); also *Solid State Commun.* **76**, 937 (1990).
- ²⁷J. Orenstein, S. Schmitt-Rink, and A. Ruckenstein, in *Electronic Properties of High- T_c Superconductors and Related Compounds*, edited by H. Kuzmany, M. Mehring, and J. Fink (Springer, Berlin, 1990), p. 254.
- ²⁸D. Mandrus, L. Forro, D. Koller, and L. Mihaly (unpublished).
- ²⁹J. Liu, J. Wang, A. M. Goldman, Y. C. Chang, and P. Z. Jiang (to be published).
- ³⁰D. S. Bessau, B. O. Wells, Z. Shen, W. E. Spicer, A. Arko, R. S. List, D. B. Mitzi, and A. Kapitulnik, *Phys. Rev. Lett.* **66**, 2160 (1991).
- ³¹K. Holczer, L. Forro, L. Mihaly, and G. Grüner, *Phys. Rev. Lett.* (to be published); G. Grüner (private communication).